

## VOR—calibration by an airborne integrated navigation system

TORRE SMESTAD†

Keywords: *avionics, VOR, calibration, inertial navigation, integrated navigation Kalman filtering, sensitivity analysis, modelling errors.*

A simulation study of a possible application of modern control theory is presented. The problem is to check and calibrate a VOR-station from a circling aircraft. An accurate position estimate of the circling aircraft is needed in order to calculate the errors in the received VOR-signals. The position estimate is here obtained from an integrated navigation system using an inertial navigation system (INS), a laser range-finder, angle measurements on the laser line-of-sight, and barometer readings. The range and angle measurements are fed to a Kalman filter which estimates errors in the navigation system. Simulation results show that satisfactory accuracy is obtained by this method. The paper presents a description of the proposed system, the simulation model used, simulation results and some sensitivity analysis.

### Notation

N, E, Z = subscripts indicating North-, East-, and Azimuth-axis  
 $\delta r_N, \delta r_E$  = components of position error  
 $\delta v_N, \delta v_E$  = components of velocity error  
 $\epsilon_N, \epsilon_E, \epsilon_Z$  = platform misalignment  
 $\delta n\omega_N, \delta n\omega_E, \delta n\omega_Z$  = gyro bias errors (gyro drifts)  
 $\delta s\omega_N, \delta s\omega_E, \delta s\omega_Z$  = gyro scale-factor errors  
 $\delta na_N, \delta na_E$  = accelerometer bias errors  
 $\delta sa_N, \delta sa_E$  = accelerometer scale-factor errors  
 $\delta h_1, \delta h_2$  = altitude errors  
 $\delta R$  = bias in laser range-finder  
 $\Psi$  = azimuth of direction from VOR to aircraft  
 $\theta$  = elevation of direction from VOR to aircraft  
 $R_{VOR}$  = distance from VOR to aircraft  
 $\theta', R'_{VOR}$  = measured values of  $\Psi, \theta$ , and  $R_{VOR}$  assuming no measurement noise  
 $\Psi'', \theta'', R''_{VOR}$  = expected values of  $\Psi, \theta$ , and  $R_{VOR}$   
 $v_N, v_E$  = velocity components of aircraft  
 $r$  = earth radius  
 $\omega_{ei}$  = earth rate  
 $L$  = latitude

### 1. Introduction

This paper presents a simulation study of a possible application of modern control theory. The investigations constituted the thesis work for the Cand real degree at the University of Oslo (Smestad 1976). The work was carried out at the Norwegian

† Norwegian Defence Research Establishment, N-2007 Kjeller, Norway.

Defence Research Establishment (NDRE) at Kjeller from January 1974 to May 1976. The objective of the investigation was

'to find out whether a satisfactory calibration accuracy of a VOR-station can be obtained by applying a Kalman filtering technique to the information from an INS, VOR/DME-station, and start and landing position of the aircraft, with a possible use of a laser range-finder.'

In addition to being the groundwork for a thesis, the investigations should serve two purposes: to give the Directorate of Civil Aviation in Norway information about possible calibration methods of VOR-stations; and to support the experience at NDRE in the area of inertial navigation and Kalman filtering.

## 2. Problem formulation

VOR-stations (VHF Omnidirectional Range) are used world-wide for *en-route* navigation of civil aircraft (Kayton and Fried 1969). They supply listening aircraft with information about the direction to the VOR-station. The normal accuracy is  $1-2^\circ$  of arc, but errors may become several times as large. The VOR-stations are subject to regular checks and calibration for safety reasons. VOR-stations are normally combined with a DME (Distance Measuring Equipment).

The principle of the calibration method currently being used, is shown in Fig. 1. A reference direction is obtained by a ground-mounted theodolite. The operator on the ground reports the reference direction up to the aircraft, where it is compared with the received VOR-signals. The accuracy of this method is  $0.5-1^\circ$ . The authorities responsible for the operation of the VOR-stations report a need for a new calibration method. Important qualities of a new method are that it should be

- (a) inexpensive,
- (b) quick and simple to operate,
- (c) of high accuracy,
- (d) independent of weather.

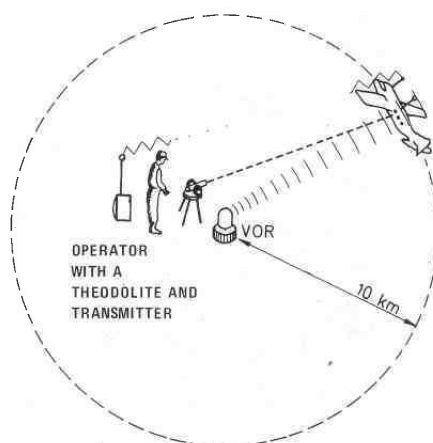


Figure 1. Principle of current VOR-calibration.

Independence of ground operated equipment has a bearing on items (a) and (b). Item (b) also has a bearing on the cost of the method because of expensive in-flight time of the calibration aircraft. Desired accuracy is  $0.1^\circ$ .

### 3. Concept of solution

The basic component in the NDRE proposal is an INS. This navigation system is self-contained in that it needs, at least in principle, no external information. An INS continuously reports position, velocity and the orientation of the vehicle, based on measurements of inertial forces (Britting 1971). Because of error build-up during operation, the errors in an INS are usually reset by means of external speed and/or position measurements. Preliminary simulations showed that the information from the start and landing position, and VOR/DME-signals was insufficient for the required accuracy. Simulation of measurements from an airborne laser range-finder produced encouraging results and the previously mentioned information became superfluous.

At a first glance, the range measurements may seem insufficient to produce an angle estimate. However, the INS 'conserves' the range information so that distance measurements taken from other viewing points will eventually produce angle information. The principle is shown in Fig. 2.

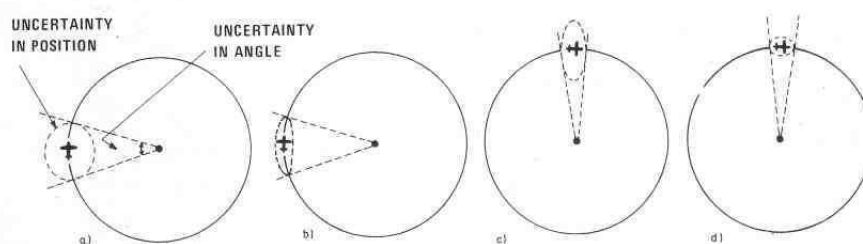


Figure 2. Angle information by range measurements and INS. Position and angle uncertainty shown (a) prior to first range measurement, (b) after first range measurement, (c) prior to second range measurement, (d) after second range measurement.

The altitude of the aircraft is needed in order to interpret the measured slant-range. Measurements of barometric pressure (corrected by ground pressure) were shown to produce altitude estimates of sufficient accuracy. Also, the direction of the laser line-of-sight was needed in order to interpret the range measurements. This caused no additional problem as the laser had in any case to be directed in azimuth and elevation. Resolver readings of a moderate accuracy was shown to be sufficient.

One is then left with measurements from the following sensors: INS; laser range-finder; two resolvers (azimuth and elevation); barometer.

The measurements from these sensors are to be integrated by Kalman filtering technique (Gelb 1974). One method is to define all these measurements as measurements in the Kalman filter sense. However, this would require too much computer capacity in addition to introducing modelling problems. A common approach is to regard the INS as a reference, and define the errors in the INS as state variables. This approach is adopted here. The measurements in the Kalman filter model are

defined as the difference between measurements from other sensors and the corresponding expected values. The expected values are calculated from the INS computers. Estimates of the INS errors are assumed fed back to the INS as alignment commands to the internal stable platform, and as compensation for gyro drifts. Also, the barometric altitude is used as a kind of reference. Therefore, only the range and angle measurements are defined as measurements in the model. This approach leads to an error model, and is especially beneficial from a computational point of view because of relative modest computer requirements. Figure 3 shows the resulting computations and information flow.

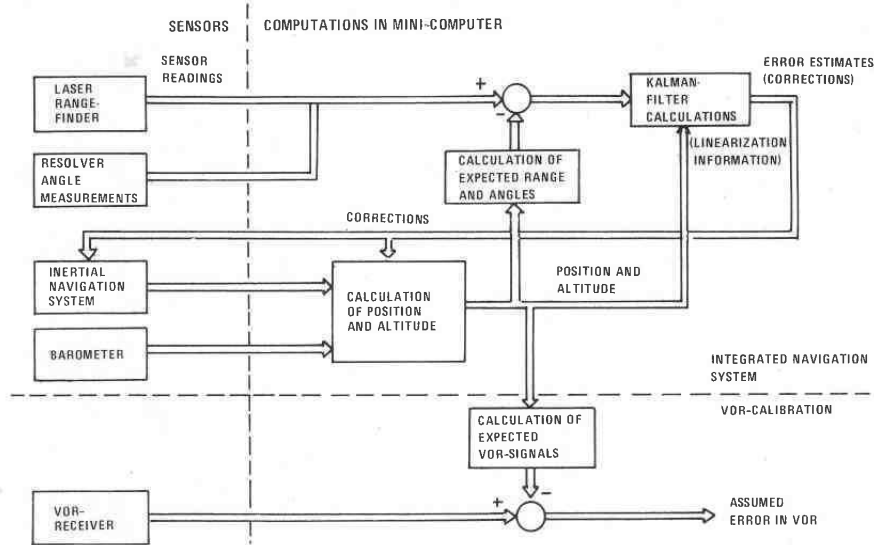


Figure 3. Calculations and information flow.

The operation of the system would proceed through the following steps:

- (1) The INS is turned on and is aligned 15–20 min before the calibration aircraft takes off.
- (2) The aircraft takes off and cruises towards the actual VOR-station; only the INS and the barometer operate.
- (3) The VOR-receiver is turned on, and set to receive from the actual VOR-station.
- (4) The aircraft starts circling the VOR-station at a distance of approximately 10 km. An operator aims the laser at the VOR by optical means, and laser-range measurements are obtained together with resolver readings (azimuth and elevation) of the laser line-of-sight.
- (5) After approximately one circuit (when the position error has become small), the real-time calculation of the VOR error is started.

- (6) After completion of the error profile (one circuit) the aircraft returns to the base or continues to another VOR-station to be checked, and then repeats the procedure.

#### 4. Evaluating methods

The calibration error is due to the position error of the integrated navigation system. The calibration accuracy has to be described statistically because of the random nature of the error sources. There are two principally different ways to obtain the statistical properties of the calibration error.

- (a) Direct calculation of the variance of the position errors north and east and transformation of the variance to the calibration error.
- (b) Repeated simulations of the calibration error by simulating the system with random errors as input (Monte-Carlo technique).

Here both methods were used with application of two standard programs, one for each method. The programs are called MULTEC (Ek and Gran 1974) and DARE (Trevor and Wait 1972). MULTEC takes as input state space equations and assumes zero-mean, Gaussian-distributed random noise. The program calculates the covariance of the state vector for optimal and sub-optimal Kalman gains. The calculated Kalman gains were stored and later used as part of the input to DARE. DARE solves a set of differential equations (linear or non-linear) by numerical integration. A fourth-order Runge-Kutta method with step-length of 1 s was used. Figure 4 shows the use of MULTEC and DARE to obtain the variance of the calibration error.

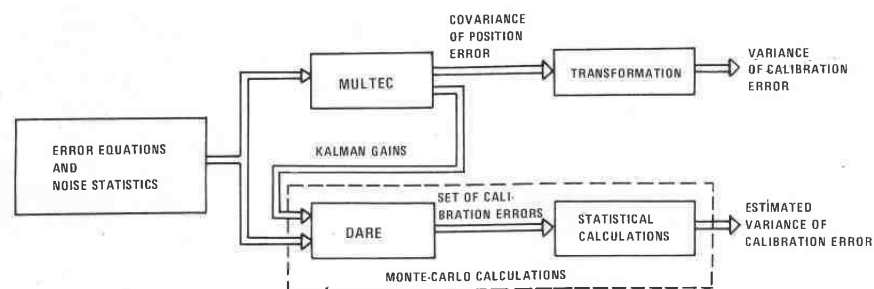


Figure 4. Use of MULTEC and DARE in the evaluation.

It should be noted that the Monte-Carlo technique allows for more detailed simulations than were performed. The underlying non-linear equations could be simulated instead of the derived linear error equations.

In a simulation study of this kind, one has to distinguish between two models, namely the computer model and the truth model. The computer model should here represent the Kalman filter model used in the implementation, while the truth model should accurately represent all vital aspects of the dynamic system. This distinction is treated to some extent. MULTEC allows covariance calculations with non-optimal Kalman gains by using the stabilized Josephson measurement update equation (Gelb 1974). Algorithms allowing more general disagreements between the two models may be found in the literature (Asher and Reeves 1975). However, none of

these was used. The equations used in DARE can generally be completely different from the ones used in MULTEC for obtaining the Kalman gains. Discretization and linearization errors were simulated this way.

### 5. Mathematical model

This section describes the mathematical model of the error-propagation resulting from the sensor measurements. No distinction is made between the computer and truth models at this stage. The error model is of the form

$$\left. \begin{aligned} \dot{\mathbf{x}} &= \mathbf{A}\mathbf{x} + \mathbf{C}\mathbf{v} \\ \mathbf{y} &= \mathbf{D}\mathbf{x} + \mathbf{w} \end{aligned} \right\} \quad (1)$$

where  $\mathbf{x}$  is a state vector,  $\mathbf{y}$  is a measurement vector,  $\mathbf{v}$  is a zero-mean, Gaussian white noise,  $\mathbf{w}$  is a zero-mean, uncorrelated, discrete Gaussian noise,  $\mathbf{A}$  is a system matrix,  $\mathbf{C}$  is a process noise coefficient matrix and  $\mathbf{D}$  is a measurement matrix.

As stated in §3, only the range and angle measurements are formulated as measurements in this model. The rest of the sensor measurements are described by the state vector.

The next section describes how the different sensor errors contribute to the state vector, and §5.2 describes how the state vector is related to the measurements. Section 5.3 specifies (1), while §5.4 lists the parameter values used.

#### 5.1. The state variables

An INS with a north-pointing, local-level mechanization is assumed used (Britting 1971). The error propagation may be represented fairly accurately by linear equations (Elsaesser 1975). The error equations are derived using a perturbation approach. These equations contain the seven state variables:  $\delta r_N$ ,  $\delta r_E$ ,  $\delta v_N$ ,  $\delta v_E$ ,  $\epsilon_N$ ,  $\epsilon_E$  and  $\epsilon_Z$ . These variables are forced by gyro and accelerometer errors. Each inertial instrument is assumed to have bias errors and scale-factor errors, one for each sensitive axis. These errors vary slowly with time and are represented as first-order Markov processes forced by white noise. As there are three sensitive gyro axes and two sensitive accelerometer axes, one gets ten state variables. These are:  $\delta n\omega_N$ ,  $\delta n\omega_E$ ,  $\delta n\omega_Z$ ,  $\delta s\omega_N$ ,  $\delta s\omega_E$ ,  $\delta s\omega_Z$ ,  $\delta na_N$ ,  $\delta na_E$ ,  $\delta sa_N$  and  $\delta sa_E$ .

The pressure sensed by the barometer must be transformed to altitude. Only the error in the altitude indication is modelled. This error is caused both by error in the measurement of pressure and of the interpretation of pressure in terms of altitude above the ground. The last error source is mainly due to imprecise knowledge of the current ground pressure and atmosphere. These two error sources are modelled as first-order Markov processes forced by white noise. They have different time constants and magnitude. The state variables are  $\delta h_1$  and  $\delta h_2$ .

The Norwegian laser range-finder SIMRAD LP3 is assumed used. The range is measured by observing the time-period between an emitted laser pulse and the reflection. Errors in the range indication are mainly caused by descretion noise of the time-measurements. This error is uncorrelated, that is, independent, between measurements, and is included as measurement noise in the model. Varying intensity of the reflected laser pulse will introduce an error. This error is correlated since the target is illuminated from almost the same direction in subsequent measurements. This error is represented by a first-order Markov process forced by white noise. The state variable is  $\delta R$ .

The error in the angle measurement is caused by imprecise aiming of the laser line-of-sight and of resolver errors. These errors are included as measurement noise since they are assumed uncorrelated.

### 5.2. The measurements

Only range and angles are included as measurements in the model. The measurements are defined as the difference between the received measurements of range and angles and the corresponding expected measurements based on the output from the INS. One obtains

$$y_1 = R'_{\text{VOR}} - R''_{\text{VOR}} + w_1$$

$$y_2 = \Psi'' - \Psi' + w_2$$

$$y_3 = \theta' - \theta'' + w_3$$

where  $y_1, y_2, y_3$  and  $w_1, w_2, w_3$  are the components of  $y$  and  $w$  in (1). These equations are non-linear in the state variables, and have to be linearized. The element  $d_{ij}$  of the matrix  $D$  in (1) is given by

$$d_{ij} = \left( \frac{\partial y_i}{\partial x_j} \right) \quad (2)$$

the derivation being performed where the measurement is obtained (the  $d_{ij}$ s are functions of the position of the aircraft relative to the VOR-station). The expressions for the  $d_{ij}$ s in (2) may be identified by a careful geometrical inspection of Fig. 5.

As may be seen, the following state variables contribute to the measurements:  $\delta r_N, \delta r_E, \epsilon_N, \epsilon_E, \epsilon_Z, \delta h_1, \delta h_2$  and  $\delta R$ .

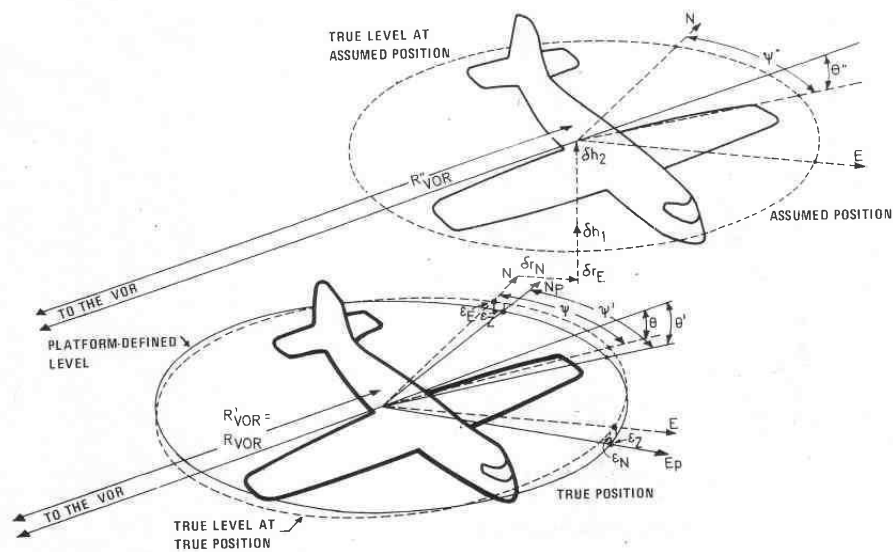


Figure 5. Variables involved in the measurements.

Noting that an error is defined by the equation

$$V_c = V_t + \delta V$$

where  $V_c$  is computed value,  $V_t$  is true value, and  $\delta V$  is the error, one gets the following expressions for the elements in the measurement matrix:

$$\begin{aligned} \frac{\partial y_1}{\partial \delta r_N} &= -\cos \theta \cdot \cos \Psi, & \frac{\partial y_1}{\partial \delta r_E} &= -\cos \theta \cdot \sin \Psi \\ \frac{\partial y_1}{\partial \delta h_1} &= \frac{\partial y_1}{\partial \delta h_2} = \sin \theta \quad (\sin \theta < 0), & \frac{\partial y_1}{\partial \delta R} &= 1 \\ \frac{\partial y_2}{\partial \delta r_N} &= \frac{\sin \Psi}{R_{\text{VOR}} \cdot \cos \theta}, & \frac{\partial y_2}{\partial \delta r_E} &= -\frac{\cos \Psi}{R_{\text{VOR}} \cdot \cos \theta}, & \frac{\partial y_2}{\partial \epsilon_Z} &= -1 \\ \frac{\partial y_3}{\partial \delta r_N} &= \frac{\sin \theta \cdot \cos \Psi}{R_{\text{VOR}}}, & \frac{\partial y_3}{\partial \delta r_E} &= \frac{\sin \theta \cdot \sin \Psi}{R_{\text{VOR}}} \\ \frac{\partial y_3}{\partial \epsilon_N} &= -\sin \Psi, & \frac{\partial y_3}{\partial \epsilon_E} &= \cos \Psi, & \frac{\partial y_3}{\partial \delta h_1} = \frac{\partial y_3}{\partial \delta h_2} &= \frac{\cos \theta}{R_{\text{VOR}}} \end{aligned}$$

$\partial y_2 / \partial \epsilon_N$  and  $\partial y_2 / \partial \epsilon_E$  are generally non-zero, but are negligibly small.

### 5.3 State space equations

Equations (1) have the structure

$$\begin{aligned} \begin{bmatrix} x_1 \\ x_2 \\ x_3 \end{bmatrix} &= \begin{bmatrix} A_{11} & A_{12} & 0 \\ 0 & A_{22} & 0 \\ 0 & 0 & A_{33} \end{bmatrix} \begin{bmatrix} x_1 \\ x_2 \\ x_3 \end{bmatrix} + \begin{bmatrix} 0 & 0 \\ C_{12} & 0 \\ 0 & C_{23} \end{bmatrix} \begin{bmatrix} v_1 \\ v_2 \end{bmatrix} \\ \begin{bmatrix} y_1 \\ y_2 \\ y_3 \end{bmatrix} &= [D_1 \quad 0 \quad D_3] \begin{bmatrix} x_1 \\ x_2 \\ x_3 \end{bmatrix} + \begin{bmatrix} w_1 \\ w_2 \\ w_3 \end{bmatrix} \end{aligned} \quad (3)$$

where the state vector  $x^T = (x_1^T x_2^T x_3^T)$  is defined as

$$\begin{aligned} x_1^T &= (\delta r_N \delta r_E \delta v_N \delta v_E \epsilon_N \epsilon_E \epsilon_Z)^T \\ x_2^T &= (\delta n \omega_N \delta n \omega_E \delta n \omega_Z \delta s \omega_N \delta s \omega_E \delta s \omega_Z \delta n a_N \delta n a_E \delta s a_N \delta s a_E)^T \\ x_3^T &= (\delta h_1 \delta h_2 \delta R)^T \end{aligned}$$



The matrices  $A_{11}$ ,  $A_{12}$ ,  $A_{22}$ ,  $A_{33}$ ,  $C_{12}$ ,  $C_{23}$ ,  $D_1$  and  $D_2$  are defined as follows:

$$A_{11} =$$

$$\begin{bmatrix} 0 & 0 & 1 & 0 & 0 & 0 & 0 \\ 0 & 0 & 0 & 1 & 0 & 0 & 0 \\ 0 & 0 & 0 & 0 & 0 & g & a_E \\ 0 & 0 & 0 & 0 & -g & 0 & -a_N \\ -\frac{1}{r} \omega_{ei} \sin L & 0 & 0 & \frac{1}{r} & 0 & -\left(\omega_{ei} \sin L + \frac{v_E}{r} \operatorname{tg} L\right) \frac{v_N}{r} \\ 0 & 0 & -\frac{1}{r} & 0 & \left(\omega_{ei} \sin L + \frac{v_E}{r} \operatorname{tg} L\right) & 0 & \left(\omega_{ei} \cos L + \frac{v_E}{r}\right) \\ -\frac{1}{r} \left(\omega_{ei} \cos L + \frac{v_E}{r \cos^2 L}\right) & 0 & 0 & -\frac{1}{r} \operatorname{tg} L & -\frac{v_N}{r} & -\left(\omega_{ei} \cos L + \frac{v_E}{r}\right) & 0 \end{bmatrix}$$

$$A_{12} = \begin{bmatrix} 0 & 0 & 0 & 0 & 0 & 0 & 0 & 0 & 0 & 0 \\ 0 & 0 & 0 & 0 & 0 & 0 & 0 & 0 & 0 & 0 \\ 0 & 0 & 0 & 0 & 0 & 0 & 1 & 0 & a_N & 0 \\ 0 & 0 & 0 & 0 & 0 & 0 & 0 & 1 & 0 & a_E \\ 1 & 0 & 0 & \left(\omega_{ei} \cos L + \frac{v_E}{r}\right) & 0 & 0 & 0 & 0 & 0 & 0 \\ 0 & 1 & 0 & 0 & -\frac{v_N}{r} & 0 & 0 & 0 & 0 & 0 \\ 0 & 0 & 1 & 0 & 0 & -\left(\omega_{ei} \sin L + \frac{v_E}{r} \operatorname{tg} L\right) & 0 & 0 & 0 & 0 \end{bmatrix}$$

$$A_{22} = \operatorname{diag} \left( -\frac{1}{T_8}, -\frac{1}{T_9}, \dots, -\frac{1}{T_{17}} \right)$$

$$A_{33} = \operatorname{diag} \left( -\frac{1}{T_{18}}, -\frac{1}{T_{19}}, -\frac{1}{T_{20}} \right)$$

where the  $T_i$ s are the time constants of the corresponding state variables (the first-order Markov processes).  $C_{12}$  and  $C_{23}$  are identity matrices of proper dimensions.

$$D_1 = \begin{bmatrix} -\cos \theta \cdot \cos \psi & -\cos \theta \cdot \sin \psi & 0 & 0 & 0 & 0 & 0 \\ \frac{\sin \psi}{R_{\text{VOR}} \cdot \cos \theta} & \frac{-\cos \psi}{R_{\text{VOR}} \cdot \cos \theta} & 0 & 0 & 0 & 0 & -1 \\ \frac{\sin \theta \cdot \cos \psi}{R_{\text{VOR}}} & \frac{\sin \theta \cdot \sin \psi}{R_{\text{VOR}}} & 0 & 0 & -\sin \psi & \cos \psi & 0 \end{bmatrix}$$

$$D_3 = \begin{bmatrix} \sin \theta & \sin \theta & 1 \\ 0 & 0 & 0 \\ \frac{\cos \theta}{R_{\text{VOR}}} & \frac{\cos \theta}{R_{\text{VOR}}} & 0 \end{bmatrix}$$

Note that the matrices  $A_{11}$ ,  $A_{12}$ ,  $D_1$  and  $D_3$  are time-varying. Their time-varying elements are functions of the aircrafts position relative to the VOR-station and the velocity of the aircraft.

#### 5.4. Parameter values

The nominal parameter values are listed in the subsequent tables. Table 1 specifies the parameter values of the state variable represented by first-order Markov processes. Table 2 specifies the measurement noise, Table 3 the initial covariance, and Table 4 the important remaining parameters for performing a simulation of the integrated navigation system.

State variable	Time constant	Standard deviation
$\delta n\omega_{N, E, Z}$	5 hours	$1.1 \times 10^{-7} \text{ rad s}^{-1}$ (1.5 meru)
$\delta s\omega_{N, E, Z}$	5 hours	0.002
$\delta na_{N, E}$	3 hours	$0.001 \text{ ms}^{-2}$
$\delta sa_{N, E}$	3 hours	0.001
$\delta h_1$	5 s	5 m
$\delta h_2$	3 hours	25 m
$\delta R$	3 min	1 m

Table 1. Specification of the first-order Markov processes

Measurement	Standard deviation
Range	5 m
Azimuth	$3.5 \times 10^{-3} \text{ rad}$ ( $0.2^\circ$ )
Elevation	$3.5 \times 10^{-3} \text{ rad}$

Table 2. Specification of measurement noise

State variable	Standard deviation
$\delta r_N, \delta r_E$	3000 m
$\delta v_N, \delta v_E$	$0.9 \text{ ms}^{-1}$
$\epsilon_N, \epsilon_E$	0.15 mrad
$\epsilon_Z$	3.6 mrad

Table 3. Initial uncertainty. (The initial uncertainty of the states modelled as first-order Markov processes are equal to Table 1 values.)

Parameter	Value
Circling radius ( $R_{\text{VOR}}$ )	10000 m
Circling direction	clockwise
Altitude above VOR	1000 m
Speed of aircraft	$113.2 \text{ ms}^{-1}$ (220 knots)
Time between measurements	30 s

Table 4. Specification of simulation parameters

## 6. Simulation results

### 6.1. Expected calibration accuracy

The application of a Kalman filter to the error model (3) does not require excessive computer capacity. An optimal Kalman filter is therefore assumed. Figure 6 shows a plot of the position errors North and East during two circuits when the model and parameter values from the previous section are used. The position of the aircraft relative to the VOR-station is associated with the time axis.

The standard deviation of the calibration error is easily calculated from the standard deviation of the position errors when the aircraft is due North, East, South or West of the VOR. Figure 7 shows the result and Fig. 8 shows the calibration accuracy calculated by the Monte-Carlo technique.

### 6.2. Sensitivity analysis

The purpose of the sensitivity analysis was to investigate the importance of the different parameters with respect to calibration accuracy, and identify possible crucial parameters. Such an analysis would therefore give valuable information about requirements for the different sensors. It would also give information about how to operate the calibration aircraft in terms of speed, altitude and range from the VOR in order to make efficient use of the sensors and to reduce costs.

One should distinguish between two measures of parameter sensitivity. One measure is obtained when the optimal Kalman gains are used for all parameter values. The other is obtained when the Kalman gains are fixed as the parameters vary, which implies modelling error. Both kinds of sensitivity analysis were to some extent performed, the latter is referred to as the modelling error in the subsequent sections.

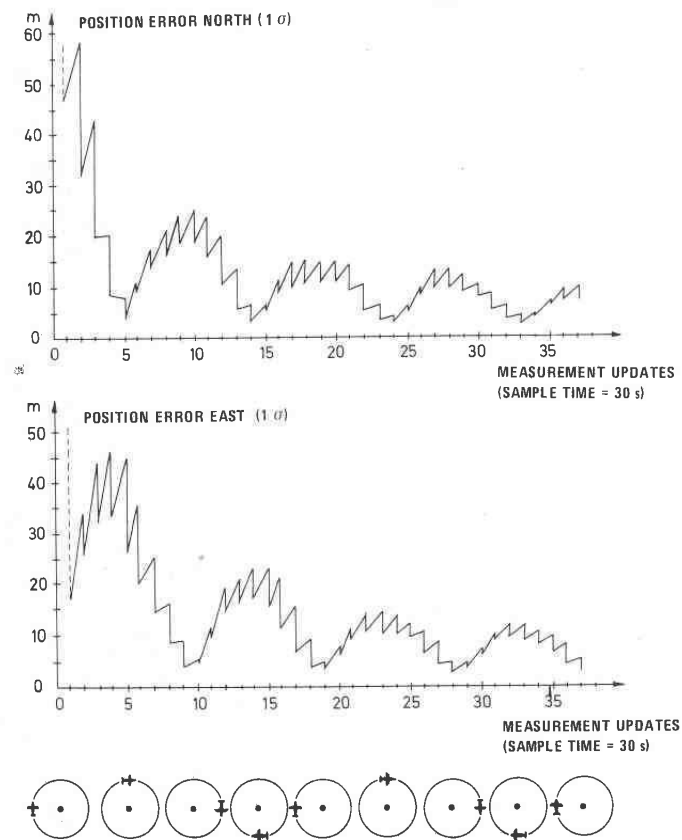


Figure 6. Position errors North and East.

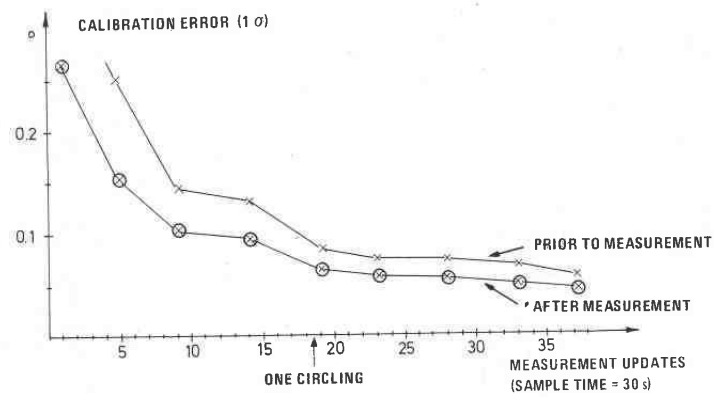


Figure 7. Calibration error calculated by covariance analysis.

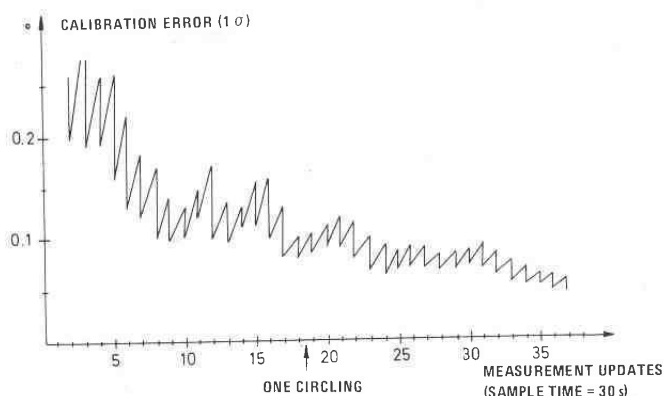


Figure 8. Calibration error calculated by the Monte-Carlo technique.

(a) *INS*

The quality of the inertial instruments (gyros and accelerometers) is crucial both to the performance of an INS and to its price. When increasing the gyro and accelerometer errors by a factor of three, the calibration error increased by a factor of two when using an optimal Kalman filter, and increased by a factor of three when using the nominal Kalman filter (optimal for the parameters listed in §5.4). These results show that the quality of the INS and a proper modelling of its errors are essential.

(b) *The laser range-finder*

As mentioned in §5.1, the dominant error is the discretization error of the time measurements. The probability density has a triangular form, resulting from the convolution of two uniform distributions. The Kalman filter assumes Gaussian distribution of all errors, but simulations showed negligible sensitivity to this modelling error.

Diagram (a) in Fig. 9 shows the sensitivity to the magnitude of this error when optimal Kalman gains are used. As seen, the accuracy of the range measurements should be within 5 m. Simulations showed that laser pulses reflected from objects near the VOR-stations could produce large calibration errors. Tests on the received range measurements for rejecting outliers were not able to prevent large calibration errors. It is therefore essential that the range is measured to the correct object.

(c) *Angle measurements*

The errors of the azimuth and elevation measurements were assumed uncorrelated. A bias error in the azimuth measurement introduced a bias in the calibration error. The magnitude of the latter was approximately half the magnitude of the measurement bias when not modelled. The inclusion of the bias in the Kalman filter did not improve the calibration error significantly. Reducing the random measurement errors of the angles by a factor of three, only reduced the calibration accuracy by about 30%.

(d) *Manoeuvres*

The manoeuvre investigations included speed, range from VOR, altitude and use of other circuit patterns. The results of the sensitivity to speed and range from the

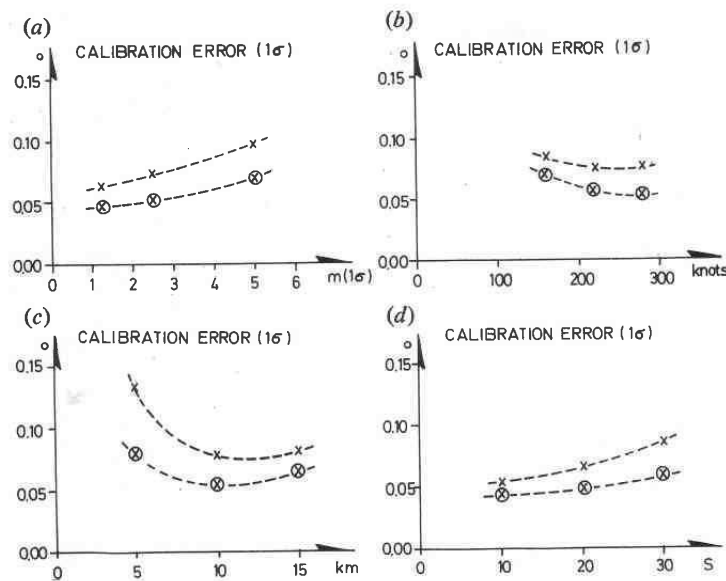


Figure 9. Sensitivity plots, optimal Kalman gains. The calibration accuracy after  $1\frac{1}{2}$  circles as a function of (a) random error in range measurements, (b) speed of aircraft, (c) range from VOR (radius of circle), (d) time between measurement updates;  $\times$ —prior to measurement update,  $\otimes$ —after measurement update.

VOR are shown in the diagrams (b) and (c) of Fig. 9. Greater altitude reduced the calibration accuracy, but not significantly for altitudes below 2000 m. Patterns, other than a circle with the VOR as centre, were investigated but did not produce better calibration accuracy.

#### (e) Frequency of the measurements

As stated, only the range and angle measurements are defined as Kalman filter measurements. Higher measurement frequency means higher computer load and increased calibration accuracy. Diagram (d) in Fig. 9 shows the sensitivity results. If the measurements are lost during one quarter of the circle, for example because of a cloud, the calibration error may become two to three times as large during the blank period, but the accuracy is quickly regained when new measurements arrive.

#### (f) Linearization and discretization

As stated in §5.3, the system matrix  $A$  and the measurement matrix  $D$  are time varying, the latter evolved from linearization. Consequently, linearization and discretization errors are introduced. The linearization of the measurements assumes knowledge of the altitude and position of the aircraft relative to the VOR-station, which are not exactly known by the integrated navigation system. The investigations indicated that the resulting linearization errors were not serious. However, a systematic position error of more than 50 m could produce significant effects on the calibration error. The time-varying  $A$ -matrix has to be represented by a sequence of slightly different transition matrices. This approximation introduced no noticeable

effects, in fact a constant transition matrix (assuming no velocity of the aircraft) was shown to be a satisfactory approximation.

## 7. Conclusion

A simulation study of a new calibration method for VOR-stations is presented. The method is independent of ground equipment. The position of the circling aircraft, and thereby the reference direction to the VOR-station, is essentially obtained by INS and range measurements to the VOR by a laser range-finder. These sensors together with barometric altitude and angle measurements on the laser line-of-sight are integrated by Kalman filtering techniques using a minicomputer. Covariance and Monte-Carlo simulations of the systems error equations show that a calibration accuracy of about  $0.1^\circ$  may be obtained, which is about ten times better than the method currently employed. Important conclusions from the sensitivity analysis are that the quality of the INS is fairly important, that the range accuracy should be within 5 m and that linearization errors of the measurements seem to be negligible.

Simplification of the 20th-order Kalman filter is not investigated, but one could expect that a 10th- or 12th-order Kalman filter will produce sufficiently accurate estimates.

## REFERENCES

- ASHER, R. B., and REEVES, R. M. (1975). Performance evaluation of suboptimal filters. *I.E.E.E. Trans. Aerospace Electron. Syst.*, **11**, 400-405.
- BRITTING, K. R. (1971). *Inertial Navigation Systems Analysis* (Wiley-Interscience).
- EK, A., and GRAN, E. (1974). Program MULTEC-1, Multivariable Estimation and Control, Institutt for Atomenergi, Norway.
- ELSAESSER, W. R. (1975). Error propagation in the ship's inertial navigator; linear vs non-linear theory, and the effects of ship's velocity and earth's oblateness, U.S. Naval Weapons Laboratory, Dahlgren, Virginia, U.S.A.
- GELB, A. (1974). *Applied Optimal Estimation* (MIT Press).
- KAYTON, M., and FRIED, W. R. (1969). *Avionics Navigation Systems* (Wiley).
- SMESTAD, T. (1976). Kalibrering av radionavigasjonshjelpemidlet VOR ved hjelp av treghetsnavigasjon, Norwegian Defence Research Establishment, Kjeller, Norway.
- TREVOR, A. V., and WAIT, J. V. (1972). DARE 111B users manual, University of Arizona, U.S.A.